

A Wolf-Rayet/black-hole X-ray binary candidate in NGC 300

S. Carpano¹, A.M.T. Pollock¹, J. Wilms², M. Ehle¹, and M. Schirmer³

¹ XMM-Newton Science Operations Centre, ESAC, European Space Agency, Apartado 50727, 28080 Madrid, Spain

² Dr. Remeis Sternwarte, Astronomisches Institut der FAU Erlangen-Nürnberg, Sternwartstr. 7, 96049 Bamberg, Germany

³ Isaac Newton Group of Telescopes, 38700 Santa Cruz de La Palma, Spain

Submitted: 9 October 2006; Accepted: 6 November 2006

ABSTRACT

Context. Wolf Rayet/black hole binaries are believed to exist as a later evolutionary product of high-mass X-ray binaries. Hundreds of such binaries may exist in galaxies, but only a few of them are close enough to be observed as X-ray binaries. Only a couple of candidates have been reported so far.

Aims. Based on *XMM-Newton* observations, we report the positional coincidence of the brightest X-ray source in NGC 300 (NGC 300 X-1) with a Wolf-Rayet candidate. Temporal and spectral analysis of the X-ray source is performed.

Methods. We determine an accurate X-ray position of the object, and derive light curves, spectra and flux in four *XMM-Newton* observations.

Results. The positions of the X-ray source and the helium star candidate coincide within $0'.11 \pm 0'.45$. The X-ray light curves show irregular variability. During one *XMM-Newton* observation, the flux increased by about a factor of ten in 10 hours. The spectrum can be modelled by a power-law with $\Gamma \sim 2.45$ with additional relatively weak line emission, notably around 0.95 keV. The mean observed (absorbed) luminosity in the 0.2–10 keV band is $\sim 2 \times 10^{38}$ erg s⁻¹.

Conclusions. NGC 300 X-1 is a good candidate for a Wolf-Rayet/black-hole X-ray binary: its position coincides with a Wolf-Rayet candidate and the unabsorbed X-ray luminosity reached $L_{0.2-10\text{keV}} \sim 1 \times 10^{39}$ erg s⁻¹, suggesting the presence of a black hole.

Key words. Galaxies: individual: NGC 300 – X-rays: binaries – Stars: Wolf-Rayet

1. Introduction

A helium-star/compact-object X-ray binary was suggested by van den Heuvel & de Loore (1973) and van den Heuvel (1983) to explain the nature of Cyg X-3, and discussed further by van Kerkwijk (1995). Such systems are believed to be a late evolutionary product of high-mass X-ray binaries. HMXBs are composed of an early-type star and a neutron-star or black-hole (BH) compact object. Material from the strong wind of the star is accreted onto the compact object with the emission of X-ray radiation. When the secondary star exhausts its core-hydrogen, it expands and begins to overflow its Roche-Lobe. A common envelope forms and the compact object starts to spiral in. If the hydrogen envelope is expelled before the compact object has reached the helium core, a stable binary system with a short orbital period is formed. Ergma & Yungelson (1998) showed, by means of population synthesis, that a few hundred such black holes with helium star companions may form in our galaxy. The orbital periods of the majority exceed 10 hrs, with a maximum at ~ 100 hrs. However, following Illarionov & Sunyaev (1975), the formation of accretion disks from the strong stellar wind of a Wolf-Rayet (WR) star is possible only for short orbital periods of (< 10 hrs). The number of such systems is expected to be extremely small (Ergma & Yungelson 1998).

In the Galaxy, Cyg X-3 is a good candidate for such a binary system. This X-ray source is one of the most luminous in the Galaxy with $L_X \sim 10^{38}$ erg s⁻¹ and has a Wolf-Rayet companion star designated WR 145a (van Kerkwijk et al. 1992). A second candidate, IC 10 X-1 ($L_X \sim 1.2 \times 10^{38}$ erg s⁻¹) has been observed in the starburst galaxy IC 10 (Bauer & Brandt 2004; Wang et al.

2005). Although two other much less luminous candidates in the LMC were suggested by Wang (1995) from *ROSAT* observations, Portegies Zwart et al. (2002) and Townsley et al. (2006) concluded, partially on the basis of more recent *Chandra* data, that these two objects are more likely to be colliding-wind binaries. In this paper we report the discovery of a third high-luminosity candidate for a WR/BH X-ray binary in the galaxy NGC 300.

NGC 300 is a dwarf spiral galaxy, belonging to the Sculptor galaxy group, located at a distance of ~ 1.88 Mpc (Gieren et al. 2005). Because it is almost face-on oriented and has a low Galactic column density of $N_H = 3.6 \times 10^{20}$ cm⁻² (Dickey & Lockman 1990), it is well suited for studies of stellar content. Based on deep VLT-FORS narrow-band imaging, Schild et al. (2003) detected 58 WR star candidates in the central region of the galaxy, of which 16 were already spectroscopically confirmed (Schild & Testor 1991; Breysacher et al. 1997). Their technique consisted of taking images through two interference filters with central wavelengths at 4684Å, containing WR emission lines, and at 4781Å as a continuum reference, with band widths of 66Å and 68Å, respectively. WR candidates were selected as having peak intensities of at least 6σ in the difference (4684Å–4781Å) image.

The X-ray source population of NGC 300 has been studied with *ROSAT* (Read & Pietsch 2001) and *XMM-Newton* (Carpano et al. 2005). With mean observed luminosities of $L_{0.1-2.4\text{keV}} \sim 2.2 \times 10^{38}$ erg s⁻¹ (Read & Pietsch 2001) and $L_{0.3-6.0\text{keV}} \sim 1.7 \times 10^{38}$ erg s⁻¹ (Carpano et al. 2005), the brightest X-ray source has been suggested to be a black hole of about $5M_\odot$. In this Letter, we report the positional coincidence of this source with one of the WR candidates reported by Schild et al.

(2003). We refer to the X-ray source as NGC 300 X-1 and to the Wolf-Rayet star as WR-41 following Schild et al. (2003). The remainder of the Letter is organised as follows. Section 2 briefly describes the *XMM-Newton* observations and data reduction. In Sect. 3, we report the spatial coincidence of NGC 300 X-1 and the WR 41. Temporal and spectral analysis of the *XMM-Newton* X-ray source is shown in Sect. 4, while a discussion of our results is given in Sect. 5.

2. Observations and data reduction

To date, NGC 300 has been observed four times with *XMM-Newton* on 2000 December 26 for 32 ksec EPIC-pn time; on 2001 January 01 for 40 ksec; on 2005 May 22 for 35 ksec; and on 2005 November 25 for 35 ksec during revolutions 0192, 0195, 0998 and 1092, respectively. For each observation, the EPIC-MOS (Turner et al. 2001) and EPIC-pn (Strüder et al. 2001) cameras were operated in full frame mode with the medium filter. The data reduction was identical to that performed in our analysis of the previous *XMM-Newton* observations (Carpano et al. 2005, 2006), except that version 7.0.0 of the *XMM-Newton* Science Analysis System (SAS) and the most recent calibration files were used.

High fluxes of proton flares were observed during revolutions 0192 and 0998. After screening the MOS data for flares using the standard procedures described by the *XMM-Newton* team¹, a total of 30 ksec of low background data remained in each revolution. A more detailed description of the *XMM-Newton* data reduction can be found in Carpano et al. (2005) for the first two *XMM-Newton* observations and Carpano et al. (2006) for the last two.

3. Position coincidence of NGC 300 X-1 and WR-41

An accurate *XMM-Newton* X-ray position of NGC 300 X-1 was derived considering both statistical and systematic errors. Statistical errors depend on the brightness of the source. For a source as bright as NGC 300 X-1, they are small compared with the systematic errors in the X-ray reference frames of each observation. Although merging all four *XMM-Newton* observations would in principle reduce the statistical errors in the absence of systematic errors, we chose to use only the data of revolution 0195, where the source was bright and well separated from local instrumental features, such as chip gaps, which affected the other observations to some extent.

Initial estimates of the position of NGC 300 X-1 and its statistical error were derived using the SAS `edetect_chain` task, which performs maximum-likelihood source detection. The source was detected with a likelihood L of 44833. Probabilities P , are related to maximum likelihood values L , by the relation $P = 1 - \exp(-L)$. The statistical position error is of $0''.083$ (or $0''.077$ with the merged data). The systematic errors were tackled with the SAS task `eposcorr`, which correlates X-ray source positions with those of their optical counterparts, as explained by Carpano et al. (2005). For this, we used 12 sources inside the galaxy disk that have clear optical counterparts. The systematic shift (in the sense X-ray minus optical position) was $-1''.25 \pm 0''.28$ in right ascension and $-0''.35 \pm 0''.34$ in declination. The revised coordinates of NGC 300 X-1 are therefore $\alpha_{J2000} = 00^{\text{h}}55^{\text{m}}10^{\text{s}}.00$ and $\delta_{J2000} = -37^{\circ}42'12''.06$, with an uncertainty of $0''.45$.

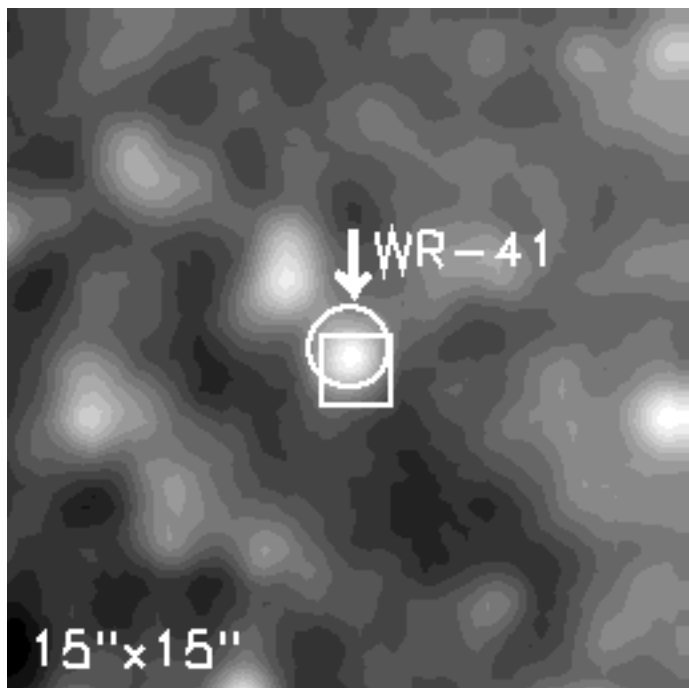


Fig. 1. $15'' \times 15''$ optical (B-band) image centred on the X-ray position of NGC 300 X-1. The circle represents the 2σ uncertainty of the X-ray position, while the box represents the position of WR-41 determined by Schild et al. (2003). North is up and East is left.

Figure 1 shows the optical (B-band) image of the field taken with the 2.2 m MPG/ESO telescope on La Silla. See Carpano et al. (2005) and Schirmer et al. (2003) for a description of the optical data and their reduction. The circle represents the 2σ uncertainty of the X-ray position, while the box is centred on the position of WR-41, derived by Schild et al. (2003). We redetermined the coordinates of the Wolf-Rayet star in the broad B-band image, using the IDL `find` routine, which is part of the `idlphot` photometry library² implemented from an early Fortran version of the DAOPHOT aperture photometry package (Stetson 1987). The revised coordinates of WR-41 are $\alpha_{J2000} = 00^{\text{h}}55^{\text{m}}09^{\text{s}}.99$ and $\delta_{J2000} = -37^{\circ}42'12''.16$. The absolute astrometric accuracy of the optical image is about $0''.25$. The difference between the position of NGC 300 X-1 and the revised position of WR-41 is thus $0''.11 \pm 0''.51$ (or $0''.52$ using the position of Schild et al. (2003)). The spatial coincidence is comparable to that found for IC 10 X-1, ($0''.23 \pm 0''.30$, Bauer & Brandt 2004), which lies at a distance of 0.8 Mpc.

4. Timing and spectral analysis of NGC 300 X-1

Figure 2 shows the *XMM-Newton* light curves of NGC 300 X-1 separately for revolutions 0192, 0195, 0998 and 1092, incorporating background-corrected MOS and pn data. The gaps in the data of revolutions 0192 and 0998 correspond to periods of high soft-energy proton flux. The time bin size is 300 sec. The light curve of NGC 300 X-1 is modulated by short-term (few 1000 sec), large-amplitude (factors of ~ 4 -5) variations in all four observations. The same type of short- and long-term variations has been reported for IC 10 X-1 (Bauer & Brandt 2004; Wang et al. 2005). During revolution 0195, the flux increased by a factor of 10 within 10 hrs, and the highest observed luminosity, assuming

¹ http://xmm.esac.esa.int/external/xmm_user_support/documentation/sasintro/USGfc.nasa.gov/contents.html

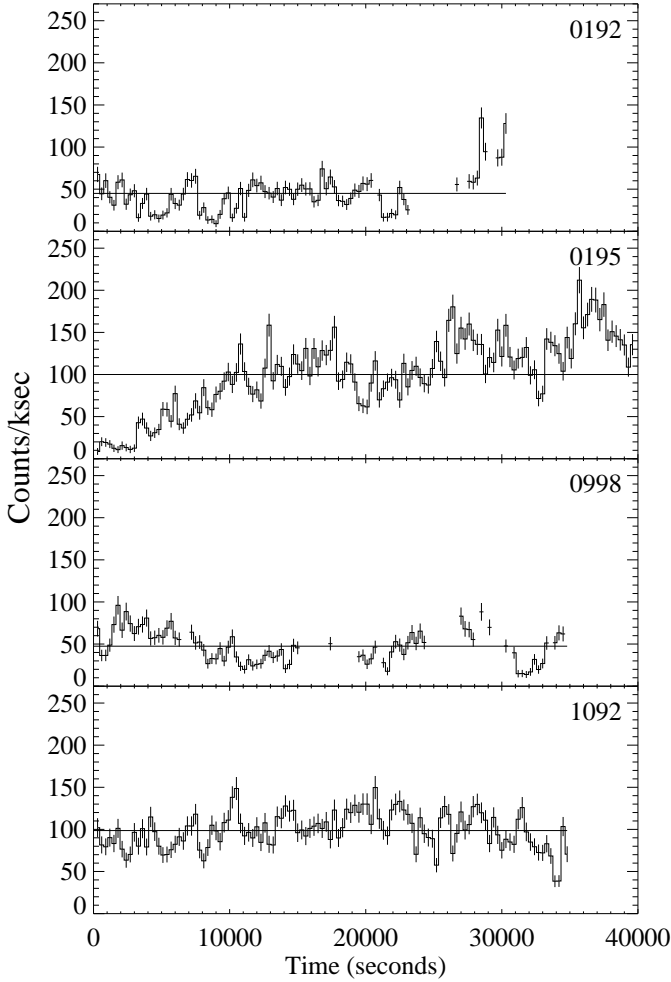


Fig. 2. EPIC-pn and -MOS 0.2–10.0 keV light curve of NGC 300 X-1 in revolutions 0192, 0195, 0998 and 1092 from top to bottom. Periods of high background have been excluded from the data. The horizontal lines show the mean values. Times start from the beginning of each observation.

isotropic emission, was $L_{0.2-10.0\text{keV}} \sim 6 \times 10^{38} \text{ erg s}^{-1}$. The corresponding unabsorbed luminosity is $\sim 1 \times 10^{39} \text{ erg s}^{-1}$. Using periodograms and epoch-folding, no short-time periodic signal was found on timescales between 5 sec and 30 ksec.

Figure 3 shows the pn and MOS spectra of NGC 300 X-1. For clarity, we have plotted the total spectra from the combination of all four observations. We first tried to fit single power-law models to the data, where parameters were left free in each observation, yielding $\chi^2_\nu/\nu = 1.32$. From the residuals shown at the bottom of Fig. 3, some excess around 0.95 keV is evident. Adding a Gaussian line significantly improved the fit, $\chi^2_\nu/\nu = 1.15$ for $\nu = 1033$ degrees of freedom. The best-fitting parameters of the absorbed combined power-law and single Gaussian-line model are shown in Table 1 for each observation separately. N_{H} is the equivalent column density of neutral hydrogen, Γ the photon index, E_{L} the energy of the line and σ_{L} its width, and Norm_{L} and Norm_{Γ} are the normalisation constants for the Gaussian line and the power-law component, respectively. The corresponding 0.2–10 keV flux, absorbed and unabsorbed luminosities are shown in the last three rows. Uncertainties are given at 90% confidence level. Allowing a variable photon index between observations does not improve the fit

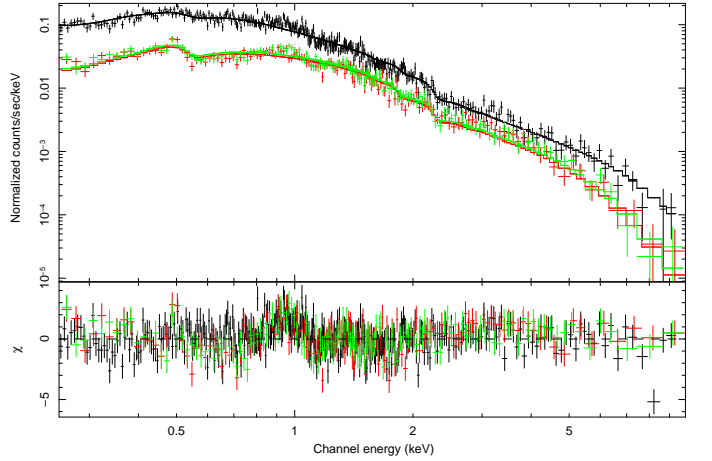


Fig. 3. EPIC-pn (black) and -MOS (red and green) spectra of NGC 300 X-1 added for the four *XMM-Newton* observations. The spectrum is fitted with an absorbed power-law model. Bottom: residuals expressed in σ . Note the excess in the residuals around 0.95 keV suggesting the presence of discrete emission.

Table 1. Results of the spectral fits for NGC 300 X-1, using an absorbed power-law model and a Gaussian line (phabs*(gauss+power), in XSPEC).

| <i>XMM-Newton</i> rev.: | 0192 | 0195 | 0998 | 1092 |
|--|------------------------|------------------------|------------------------|------------------------|
| $N_{\text{H}} (\times 10^{20} \text{ cm}^{-2})$ | $4.22^{+0.61}_{-0.71}$ | $7.84^{+0.57}_{-0.69}$ | $6.04^{+0.79}_{-0.44}$ | $7.79^{+0.60}_{-0.69}$ |
| Γ | | | $2.45^{+0.03}_{-0.03}$ | |
| $\text{Norm}_{\Gamma} \times 10^{-4}$ | $0.55^{+0.02}_{-0.02}$ | $1.43^{+0.04}_{-0.05}$ | $1.21^{+0.05}_{-0.06}$ | $1.45^{+0.05}_{-0.05}$ |
| $E_{\text{L}} \text{ (keV)}$ | | | $0.94^{+0.01}_{-0.01}$ | |
| $\sigma_{\text{L}} \text{ (keV)}$ | | | $0.07^{+0.01}_{-0.01}$ | |
| $\text{Norm}_{\text{L}} \times 10^{-5}$ | < 0.10 | $1.13^{+0.35}_{-0.18}$ | $1.00^{+0.39}_{-0.32}$ | $1.60^{+0.30}_{-0.29}$ |
| $F_{0.2-10\text{keV}} \times 10^{-13} \text{ (cgs)}$ | $2.36^{+0.14}_{-0.16}$ | $5.40^{+0.19}_{-0.21}$ | $4.87^{+0.29}_{-0.30}$ | $5.56^{+0.23}_{-0.23}$ |
| $L_{0.2-10\text{keV}}^{\text{obs}} \times 10^{38} \text{ (cgs)}$ | $1.00^{+0.06}_{-0.07}$ | $2.29^{+0.08}_{-0.09}$ | $2.06^{+0.12}_{-0.13}$ | $2.35^{+0.10}_{-0.10}$ |
| $L_{0.2-10\text{keV}}^{\text{unabs}} \times 10^{38} \text{ (cgs)}$ | $1.43^{+0.05}_{-0.12}$ | $3.75^{+0.06}_{-0.21}$ | $3.18^{+0.11}_{-0.26}$ | $3.85^{+0.08}_{-0.22}$ |

or change spectral parameters within the errors except for revolution 0998, where $N_{\text{H}} = 4.78^{+1.06}_{-1.36} \times 10^{20} \text{ cm}^{-2}$ and $\Gamma = 2.35^{+0.08}_{-0.09}$.

The mean observed luminosity increased by more than a factor of two from the lowest state in revolution 0192 to the highest in revolution 1092. When the source was brighter, the intrinsic absorption, as well as the emission line/continuum ratio, increased. In revolution 0192, the equivalent hydrogen column, N_{H} , was compatible with the galactic value ($N_{\text{H}} = 3.6 \times 10^{20} \text{ cm}^{-2}$), implying little or no intrinsic absorption in the low state.

We also tried to fit the data using a power-law model combined with thermal emission from a collisionally ionized plasma modelled by *apec* in XSPEC (version 11.3.2). This thermal emission includes both lines and continuum emissivities with a best-fit temperature of $\sim 0.86^{+0.03}_{-0.04} \text{ keV}$. This model is statistically indistinguishable from the power-law plus Gaussian line model.

5. Discussion

WR-41 is a Wolf-Rayet candidate discovered by Schild et al. (2003). Using narrow band imaging techniques, they measured that the flux of the source at $\lambda = 4684 \pm 66 \text{ \AA}$, where strong WR emission lines are observed, has an excess of 0.95 mag over

the continuum. Its relative magnitude is $m_V = 22.44$ mag, which corresponds, at a distance of 1.88 Mpc, to an absolute magnitude of -3.93 mag. Following Schild et al. (2003), objects such as WR-41 are candidates for weak-line single WN-type stars.

We have shown in this Letter that the brightest X-ray source in the nearby galaxy NGC 300, NGC 300 X-1, is likely to be the X-ray counterpart of WR-41. This would imply that the system is a good candidate for membership in the rare class of WR/BH X-ray binaries. Irregular flux variations were observed in the four light curves, with a particularly large increase observed over about 10 hours during *XMM-Newton* revolution 0195. The origin of these variations is not clear, but likely due to variations in the accretion rate and/or variable absorption in the strong stellar wind of the donor star. We also note that no obvious eclipse is visible in any of the light curves. As WR/BH X-ray binaries should have small orbital periods < 10 hrs, we interpret the absence of eclipses as a possible indication of face-on orientation of the system.

In the context of a WR/BH X-ray binary, the weak discrete emission observed in the spectra of NGC 300-X-1, which is likely to be composed of several unresolved lines, may arise from reprocessing by the photoionized stellar wind: the X-rays emitted around the black hole are ionizing the high density wind of the Wolf-Rayet star. This may explain why this emission is more pronounced when the X-ray flux is higher. The dense wind is probably also responsible for the intrinsic absorption that increases as the X-ray source gets brighter. Similar ideas explain the weak emission lines observed in Cyg X-3 (e.g., Kawashima & Kitamoto 1996; Paerels et al. 2000) and in other wind accretors. Faint lines have also been observed in the X-ray spectrum of the candidate IC 10 X-1 (Bauer & Brandt 2004). We note that the contribution of the WR star to the X-ray flux is negligible as typical X-ray luminosities are about 10^{32} erg s $^{-1}$ for single stars and 10^{34} erg s $^{-1}$ for binaries (e.g., Pollock 1987).

To conclude, NGC 300 X-1 and WR-41 are good candidates for membership in the very rare class of Wolf-Rayet/black hole X-ray binaries. This conclusion is supported by the spatial coincidence of the sources as well as the high maximum X-ray luminosity near 10^{39} erg s $^{-1}$. As the nature of WR-41 currently relies on narrow-band photometric techniques, we encourage optical observers to acquire the spectra necessary to confirm the identification of WR-41 as a Wolf-Rayet star.

Acknowledgements. This paper is based on observations obtained with *XMM-Newton*, an ESA science mission with instruments and contributions directly funded by ESA Member States and NASA, and on observations made with ESO Telescopes at the La Silla observatory and retrieved from the ESO archive.

References

- Bauer, F. E. & Brandt, W. N. 2004, *ApJ*, 601, L67
 Breysacher, J., Azzopardi, M., Testor, G. & Muratorio, G. 1997, *A&A*, 326, 976
 Carpano, S., Wilms, J., Schirmer, M., & Kendziorra, E. 2005, *A&A*, 443, 103
 Carpano, S., Wilms, J., Schirmer, M., & Kendziorra, E. 2006, *A&A*, in press
 de Vaucouleurs, G., de Vaucouleurs, A., Corwin, jr., H., et al. 1991, *Third Catalogue of Bright Galaxies* (New York: Springer)
 Dickey, J. M. & Lockman, F. J. 1990, *ARA&A*, 28, 215
 Ergma, E. & Yungelson, L. R. 1998, *A&A*, 333, 151
 Gieren, W., Pietrzyński, G., Soszyński, I., Bresolin, F., Kudritzki, R.-P., Minniti, D. & Storm, J. 2005, *ApJ*, 628, 695
 Illarionov, A. F. & Sunyaev, R. A., *A&A*, 39, 185
 Kawashima, K. & Kitamoto, S. 1996, *PASJ*, 48, L113
 Paerels, F., Cottam, J., Sako, M., Liedahl, D. A. et al. 2000, *ApJ*, 533, L135
 Pollock, A. M. T., 1987, *ApJ*, 320, 283
 Portegies Zwart, S. F., Pooley, D. & Lewin, W. H. G., 2002, *ApJ*, 574, 762
 Read, A. M. & Pietsch, W. 2001, *A&A*, 373, 473
 Schild, H., Crowther, P. A., Abbott, J. B., & Schmutz, W. 2003, *A&A*, 397, 859
 Schild, H. & Testor, G. 1991, *A&A*, 243, 115

- Schirmer, M., Erben, T., Schneider, P., et al. 2003, *A&A*, 407, 869
 Stetson, P. B. 1987, *PASP*, 99, 191
 Strüder, L., Briel, U., Dennerl, K., et al. 2001, *A&A*, 365, L18
 Townsley, L. K., Broos, P. S., Feigelson, E. D., Garmire, G. P. & Getman, K. V. 2006, *AJ*, 131, 2164
 Turner, M. J. L., Abbey, A., Arnaud, M., et al. 2001, *A&A*, 365, L27
 van den Heuvel, E. P. J. & de Loore, C., 1973, *A&A*, 25, 387
 van den Heuvel, E.P.J. 1983, Lewin W.H.G. & van den Heuvel E.P.J. (eds), *Accretion-driven Stellar X-ray sources* (Cambridge: Cambridge Univ. Press), p. 303
 van Kerkwijk, M. H., Charles, P. A., Geballe, T. R., King, D. L., et al. 1992, *Nature*, 355, 703
 van Kerkwijk, M. H. 1995, van der Hucht, K. A. & Williams, P. M. (eds), *IAU Symposium*, 163, 527
 Wang, Q. D. 1995, *ApJ*, 453, 783
 Wang, Q. D., Whitaker, K. E. & Williams, R., 2005, *MNRAS*, 362, 1065

List of Objects

- ‘Cyg X-3’ on page 1
 ‘IC 10’ on page 1
 ‘NGC 300’ on page 1
 ‘NGC 300 X-1’ on page 1
 ‘IC 10 X-1’ on page 2